A&A 648, A96 (2021)
https://doi.org/10.1051/0004-6361/202039579
© B. Carry et al. 2021

Astronomy & Astrophysics

# Potential asteroid discoveries by the ESA *Gaia* mission

## Results from follow-up observations

B. Carry[1,2], W. Thuillot[1], F. Spoto[2,3], P. David[1], J. Berthier[1], P. Tanga[2], F. Mignard[2], S. Bouquillon[4], R. A. Mendez[5], J.-P. Rivet[2], A. Le Van Suu[6], A. Dell'Oro[7], G. Fedorets[8,9], B. Frezouls[10], M. Granvik[8,11], J. Guiraud[10], K. Muinonen[8,12], C. Panem[10], T. Pauwels[13], W. Roux[10], G. Walmsley[10], J.-M. Petit[14], L. Abe[2], V. Ayvazian[15,16], K. Baillié[1], A. Baransky[17], P. Bendjoya[2], M. Dennefeld[18], J. Desmars[1,19], S. Eggl[1,20], V. Godunova[21], D. Hestroffer[1], R. Inasaridze[15,16], V. Kashuba[22], Y. N. Krugly[23], I. E. Molotov[24], V. Robert[1,19], A. Simon[25,26], I. Sokolov[27], D. Souami[28,29], V. Tarady[21], F. Taris[4], V. Troianskyi[22,30], V. Vasylenko[25,26], and D. Vernet[2]

*(Affiliations can be found after the references)*

Received 2 October 2020 / Accepted 18 February 2021

**ABSTRACT**

*Context.* Since July 2014, the *Gaia* mission of the European Space Agency has been surveying the entire sky down to magnitude 20.7 in the visible. In addition to the millions of daily observations of stars, thousands of Solar System objects (SSOs) are observed. By comparing their positions, as measured by *Gaia*, to those of known objects, a daily processing pipeline filters known objects from potential discoveries. However, owing to *Gaia*'s specific observing mode, which follows a predetermined scanning law designed for stars as "fixed" objects on the celestial sphere, potential newly discovered moving objects are characterized by very few observations, which are acquired over a limited time. Furthermore, these objects cannot be specifically targeted by *Gaia* itself after their first detection. This aspect was recognized early on in the design of the *Gaia* data processing.

*Aims.* A daily processing pipeline dedicated to these candidate discoveries was set up to release calls for observations to a network of ground-based telescopes. Their aim is to acquire follow-up astrometry and to characterize these objects.

*Methods.* From the astrometry measured by *Gaia*, preliminary orbital solutions are determined, allowing us to predict the position of these potentially newly discovered objects in the sky while accounting for the large parallax between *Gaia* and the Earth (separated by 0.01 au). A specific task within the *Gaia* Data Processing and Analysis Consortium has been responsible for the distribution of requests for follow-up observations of potential *Gaia* SSO discoveries. Since late 2016, these calls for observations (nicknamed "alerts") have been published via a Web interface with a quasi-daily frequency, together with observing guides, which is freely available to anyone worldwide.

*Results.* Between November 2016 and the end of the first year of the extended mission (July 2020), over 1700 alerts were published, leading to the successful recovery of more than 200 objects. Among them, six have a provisional designation assigned with the *Gaia* observations; the others were previously known objects with poorly characterized orbits, precluding identification at the time of *Gaia* observations. There is a clear trend for objects with a high inclination to be unidentified, revealing a clear bias in the current census of SSOs against high-inclination populations.

**Key words.** minor planets, asteroids: general – celestial mechanics

## 1. Introduction

The main science driver of the European Space Agency (ESA) *Gaia* astrometric mission is the study of the structure and the dynamics of the Milky Way (Perryman et al. 2001). Building upon the heritage of Hipparcos, *Gaia* was designed to conduct a survey of the full celestial sphere (Gaia Collaboration 2016a) at an absolute precision of 25 microarcseconds (μas) for the parallax for $V = 15$ mag, solar-type stars, and 13 μas yr$^{-1}$ for the proper motion. *Gaia*'s onboard image processing detects and measures all celestial sources brighter than ≈20.7 mag in *Gaia*'s wide visible "G" filter (Jordi et al. 2010). It also measures the photometry in the G filter as well as low-resolution spectroscopy for all sources.

To achieve such accuracies, *Gaia* eliminates systematic errors by adopting the same strategy as its predecessor Hipparcos, that is, by simultaneously measuring, with high precision, the transit epochs of all sources in two fields of view separated by a wide angle of 106.5° (the "basic angle") during a continuous scan at a constant rate (period of 6 h). The practical realization (e.g., pixel scale and binning) implies a widely different astrometric precision between the "along scan" (AL) direction (tangent to the great circle scanned by the rotation) and the perpendicular "across scan" (AC) direction.

Multiple transit observations of the same portion of the sky, with varying scanning directions, are therefore required to measure the positions at the required microarcsecond precision. This is realized through the precession of the spinning axis[1] over 64 days, always pointing 45° away from the Sun. The so-called Astrometric Global Iterative Solution (AGIS) produces the astrometric model of the whole sky, corresponding to the combination of all star positions and proper motions, plus calibration parameters. For a complete description of the satellite and its operation, we refer the interested reader to Gaia Collaboration (2016b);

[1] This is required in any case to cover the entire celestial sphere.



Open Access article, published by EDP Sciences, under the terms of the Creative Commons Attribution License (https://creativecommons.org/licenses/by/4.0), which permits unrestricted use, distribution, and reproduction in any medium, provided the original work is properly cited.

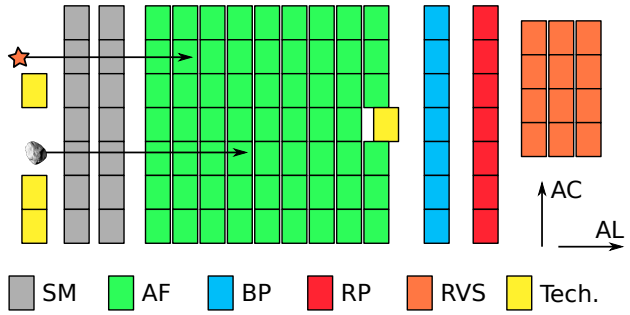


**Fig. 1.** Schematic view of the *Gaia* focal plane. Each column of CCDs is called a strip. Sources cross the focal plane in the AL direction, passing successively through the SM, the nine AFs, the BP and RP, and the RVS.

below we summarize some features that are relevant for the present work.

The two 1-m telescopes of *Gaia* are mounted on a structure that points toward the two fields separated by the basic angle and produce an image on a single focal plane. The charge-coupled devices (CCDs) that compose the focal plane operate in time-delayed integration (TDI) mode, in which electrons are moved from pixel to pixel at the same rate that the sources (and hence the photoelectrons) drift along the CCD pixel lines (i.e., in the AL direction).

*Gaia*'s focal plane contains several instruments, each corresponding to different "strips" of seven CCDs each (Fig. 1). First, the SkyMapper (SM) instrument identifies the sources from each telescope and discriminates their origin between the two fields of view using two CCD strips. This is followed by nine CCD strips for astrometry – the astrometric fields (AFs). Hereafter, "observations" refers to the positions on each of these nine CCDs, while "transit" encompasses these observations, as in Spoto et al. (2018). Then two strips provide slitless low-resolution spectroscopy, splitting the visible spectrum into a blue and a red component (i.e., a blue and a red photometer, BP and RP; Riello et al. 2018). A more restricted portion of the focal plane is devoted to the three CCD strips of the radial-velocity spectrometer (RVS; Cropper et al. 2018), collecting high-resolution spectra of bright stars ($V < 17$). With each of these 16 CCD strips containing seven CCDs each (except the three RVS strips that only contain four CCDs each) and a few technical CCDs, *Gaia*'s focal plane is the largest ever operated in space in terms of pixel numbers.

The resulting large data volume poses a challenge for telemetry. Since the start of its operations in July 2014, *Gaia* has been located at the Sun-Earth L2 Lagrangian point (0.01 au from the Earth). Upon detection by the SM, only small windows around each source are tracked along the focal plane. Most frequently, these windows only have $6 \times 12$ pixels[2]. Most of them are also binned in the AC direction such that only a unidimensional signal is transmitted to the ground. A notable exception is for sources brighter than $G < 13$ mag, for which larger 2D windows are preserved.

All the aforementioned characteristics of *Gaia* have strong consequences on its observation of Solar System object (SSO) transits including the following five examples. First, source tracking on the focal plane closely follows the rate of stars. For this reason, SSOs may drift with respect to the center of the assigned windows in the AF and ultimately leave it if the apparent velocity is large enough. A typical main-belt asteroid drifts by 1 pixel in AL during a transit over a single CCD (4.4 s) if it moves at a typical rate of 13 mas s$^{-1}$ in the same direction. Second, the motion of the SSOs produces a distortion of the signal, the shape of which is no longer well represented by a pure stellar point-spread function. Third, as a consequence, the astrometric and photometric processing must be adapted to cope with the resulting flux loss, which is variable and increases over the transit. Fourth, each measured position of an SSO is strongly constrained in the AL direction (at the 0.1–20 mas level, depending on the astrometric solution used to reduce the data; see below) but much worse in the AC direction (~600 mas). Finally, the identification of SSOs cannot be determined by the internal crossmatching of sources (which is the root of the creation of the stellar catalog; Fabricius et al. 2016) due to their motion relative to stars; it must therefore rely on a specific processing that requires an external catalog of orbits.

The potential for Solar System research with the absolute and extreme-precision astrometry, photometry, and low-resolution spectroscopy of *Gaia* was recognized early on (Mignard et al. 2007). Furthermore, early estimates considering the limiting magnitude of *Gaia* and the completeness of SSO catalogs predicted about a hundred discoveries of SSOs per week, mainly main-belt asteroids, potentially a couple of near-Earth asteroids (NEAs), and no objects in the outer Solar System (Mignard et al. 2007; Carry 2014).

While large ground-based surveys (e.g., Pan-STARRS, the Catalina Sky Survey, and the Legacy Survey of Space and Time) are expected to discover and gather multiple observations of most objects, the specific location of *Gaia* and the small solar elongation (45°) reached by its observations allows the discovery of NEAs with small aphelion distances.

Within the *Gaia* Data Processing and Analysis Consortium (DPAC), the potential for SSO discoveries led to a specific workflow for SSOs that consists of two chains. A short-term processing pipeline (named SSO-ST) runs daily to identify SSOs in the latest (72 h) transits (Tanga et al. 2016) and to trigger follow-up observations from the Earth. A ground-based follow-up network of telescopes (*Gaia*-FUN-SSO) was established to ensure observations and confirm *Gaia* discoveries (Thuillot & Dennefeld 2018). The long-term processing pipeline (named SSO-LT), which benefits from the full global astrometric solution of *Gaia*, runs on longer timescales to produce catalogs with the best astrometry, photometry, and spectroscopy of SSOs for the various data releases (DRs), the first of which with SSOs was *Gaia* DR2 (see Spoto et al. 2018).

We focus here on the results of the SSO-ST over the course of the *Gaia* nominal mission (July 2014–July 2019) and the first year of the extended mission (July 2019–July 2020). The article is organized as follows. Section 2 summarizes the main steps of the daily processing (beyond the description of the chain provided by Tanga et al. 2016). Section 3 presents the system through which calls for observations of potential discoveries are released. The network of ground-based telescopes is presented in Sect. 4, and a summary of the successful SSO recoveries is presented in Sect. 5. We discuss the orbital properties of the alerts in Sect. 6.

## 2. The SSO-ST daily processing

We briefly summarize the daily processing of *Gaia* observations in the framework of the SSO-ST. For a full description of the pipeline, we refer to Tanga et al. (2016) and *Gaia* documentation[3]. We focus here on its differences with the long-term

[2] The angular size on the sky of the pixels of the AFs is $59 \times 177$ mas.

[3] https://gea.esac.esa.int/archive/documentation/

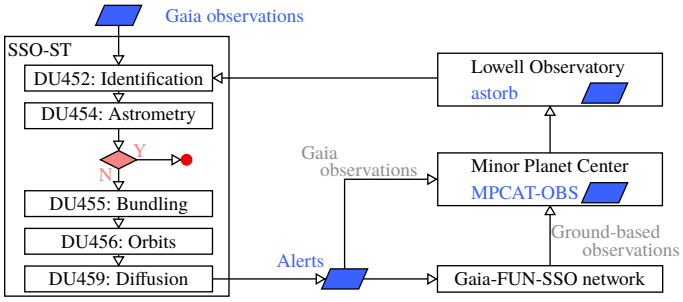


**Fig. 2.** Simplified workflow from *Gaia* observations to alert dissemination, reporting to the MPC, and update of `astorb`, the database of orbital elements used for the identification.

processing, which is thoroughly documented in Spoto et al. (2018).

An initial data treatment (IDT) of the *Gaia* data is performed upon reception on the Earth (Fabricius et al. 2016). After obtaining the signal parameters that describe the position of a source on the focal plane at the observing epoch, IDT uses a preliminary great-circle attitude solution to derive its position on the sky and executes a first crossmatching with previously observed sources. Typical sources that fail crossmatching are either artifacts (e.g., cosmic rays, diffraction spikes from bright sources, or spurious detections), sources at the limit of detection (detected only on certain transits), or transients (e.g., genuine moving objects from our Solar System). The position of the transients always changes on the sky. In all of these cases, the unmatched sources are removed from the main stellar data processing and are available for a special processing for SSOs (Fig. 2).

The first task of this processing is to identify if the source corresponds to a known SSO (task performed by the development unit DU452 of *Gaia* DPAC). All unmatched sources are potential SSO candidates. However, SSOs constitute a very minor fraction of all the sources continuously transiting the focal plane of *Gaia*. By taking the somewhat optimistic figure of 350 000 as the number asteroids that *Gaia* can observe during the entire duration of its mission, *Gaia* observes, on average, one SSO for every 4000 stars. It is clear that any inefficiency in the IDT crossmatching for stars can produce an overwhelmingly large number of false SSO detections (for instance, at a 99.9% efficiency, there are four unmatched stars for each genuine SSO).

Furthermore, a very large number of contaminants at the CCD level were found to heavily populate the sample of unmatched detections, making the task of SSO identification impossible without appropriate cleaning of the data set. The appropriate filtering was made possible by introducing the computation of the AL velocity of the source (and the AC velocity whenever possible) on the focal plane in the IDT. All sources without a detectable motion are discarded. The threshold is dynamically adjusted on the basis of the velocity distribution for each 1-day data chunk and is typically on the order of $\pm 2$ mas s$^{-1}$.

For an object that passes through the filter, its positions are checked against the predicted positions of known SSOs at the corresponding epochs. The catalog of osculating orbital elements of the minor planets, `astorb`[4] (Bowell 2014; Bailen et al. 2020), is updated on a weekly basis and the ephemerides for all SSOs are precomputed and stored in a database (this is a version of the SkyBoT software dedicated to *Gaia*; see Berthier et al. 2006, 2016, for more details). If not linked with a known SSO, the source may still be a known SSO with a poorly characterized orbit (which precludes identification), an unknown SSO, or an artifact as listed above. Because the identification relies on an external catalog, it is crucial to keep it up to date. Similarly, any bias in the current census of SSO populations will affect the identification.

A suite of different tasks is then performed one after the other on each unidentified source. The suite of observations (i.e., SM plus AF, up to ten) that defines a transit is converted into sky coordinates by DU454, after being subjected to a quality filtering to mitigate the distortion effects (due to the motion) that impair the accuracy of the centroid determination (DU453). The only attitude (the transformation from pixel coordinates to sky coordinates) available hours after the observations is the "poor" (by *Gaia* standards) Oga1 attitude, which contains many irregularities. One of the tasks of DU454 is to smooth the attitude and remove these irregularities; in doing so, it is necessary to check whether a linear motion in the sky can be fit to the transit. The obtained smoothed attitude has typical uncertainties of 25 mas in AL and 40 mas in AC, which is still much larger than the uncertainties on the high-quality Oga3 attitude that will be determined by AGIS months later (hence too late to be used for alerts) for the DRs. Next, DU454 will try to fit a linear motion on all positions of a transit as well as remove those that do not fit on the linear motion, that is, those that are either of too poor quality or are not detections of the SSO. If no linear motion can be fit at all on the transit, the entire transit is rejected and is assumed to be a contaminant.

A procedure (DU455) then attempts to link together transits in order to identify which ones belong to the same source. Based on a current census of asteroids, their typical apparent motion on the sky as a function of solar elongation (the most important parameter for this task) is determined. The linking procedure then performs an efficient search to find all possible links that satisfy this typical motion. The result is further filtered by the similarity of the measured apparent magnitude and by the compatibility of the apparent motion with the instantaneous velocity produced by the IDT. This process is applied daily to the previous 48 h' worth of data. If at least two transits are linked together, the source may be a genuine moving object. However, a few transits by *Gaia* (two or three only, in 45% and 10% of the cases, respectively, providing fewer than 6 h of observations; Tanga 2011) are not enough to compute an accurate orbital solution.

A short-arc solution, valid for a limited interval of time, is required for ground-based follow-up, which is essential to secure the orbit. The proximity of SSOs compared to the Earth–*Gaia* distance implies large parallaxes: from an arcminute for the distant Kuiper belt at 30 au from *Gaia* to over one degree for nearby (less than 0.5 au) Mars-crosser asteroids and NEAs. Because the distance of SSOs is unknown upon first observation, the parallax cannot be accounted for to convert the coordinates measured by *Gaia* into Earth-based coordinates. Preliminary orbits based on *Gaia* short arcs are thus computed within the SSO-ST (in the processing unit named DU456) to allow short-term predictions (Muinonen et al. 2016) and to guide ground-based observations. These preliminary orbits are determined through a random-walk independent sampling of ranges of SSOs. For each new source, this provides 2000 clone orbits (represented by Keplerian elements), which cover the orbital element space corresponding to a 3 $\sigma$ agreement with *Gaia* observations. We refer to Fedorets et al. (2018) for details. We estimate the uncertainty associated with these preliminary solutions by computing the area covered on sky. These uncertainties are inversely proportional to the number of transits (Fig. 3).

[4] Based on the worldwide catalog of observations maintained at the Minor Planet Center (MPCAT-OBS; Rudenko 2016).

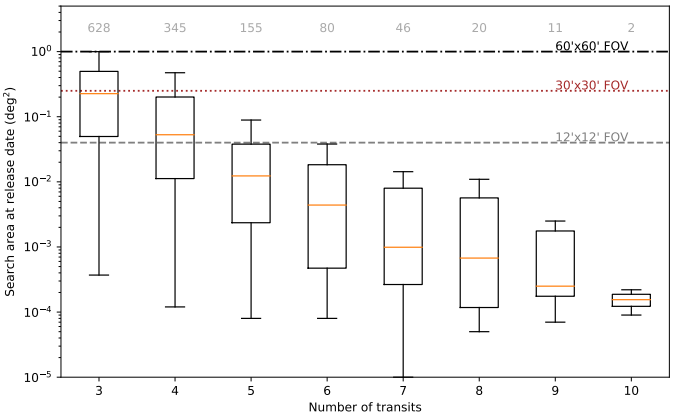


**Fig. 3.** Area on sky (presented as 25–50–75% whiskers and $3\sigma$ min, max) covered by the preliminary orbits as a function of the number of *Gaia* transits used. The gray numbers at the top correspond to the numbers of alerts released with the associated numbers of transits.

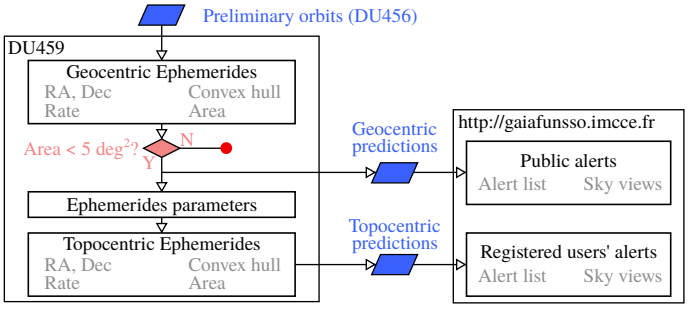


**Fig. 4.** Simplified workflow of alert processing and diffusion. Alerts are selected based on geocentric ephemerides. For each alert below the area threshold, topocentric ephemerides are computed for each observatory in the system. All ephemerides are stored in a database that is used by the Web pages.

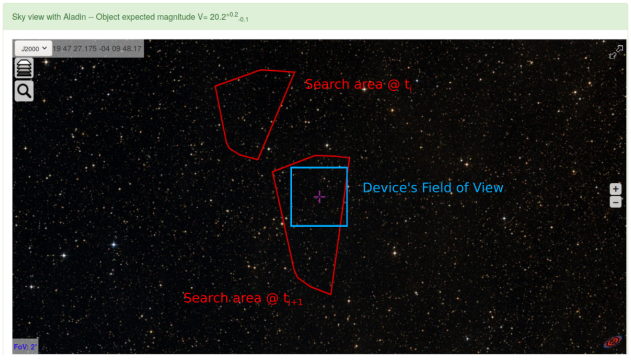


**Fig. 5.** Example of the sky view of alerts with `AladinLite`. The red polygons correspond to the convex hull of the cloud of predicted positions at different dates, and the blue square represents the field of view of the device defined by the user (only available upon registration).

These short-term orbital elements, improved by ground-based follow-up, adds enormous value to *Gaia* observations. First, without follow-up observations, these *Gaia* observations are "lost" as they cannot be linked with any known object. Second, without an orbit, the observed properties (position, apparent $G$ magnitude, and BP and RP spectra) of these asteroids cannot be appropriately studied or understood in the context of SSO populations. Such situations can arise in modern surveys and can lead to a significant loss of valuable data. As an example, the latest release (2008) of the moving object catalog of the Sloan Digital Sky Survey (Ivezić et al. 2001) contains over 470 000 observations of moving objects, of which only about 220 000 are linked with known SSOs.

The SSO-ST was set up to avoid such a situation. Its main goal is to release calls for observations ("alerts") of these unidentified sources, allowing for observations from the Earth and hence the determination of a preliminary orbit, as well as an update of the database of orbits (Fig. 2).

The pre-launch plans for the SSO-ST were to process all SSOs with at least two transits by *Gaia*. The majority of cases represent the situation where only two transits exist for an object. However, the spread of orbital solutions for these cases typically results in a large spread of solutions on the sky. This renders any follow-up efforts unfeasible. Therefore, we operate the pipeline for objects with a minimum of three transits (Fig. 3).

## 3. The alert release interface

An interface to release the calls for observations (alerts) to the community of observers was set up. This is the last task of the SSO-ST (DU459), the workflow of which is described in Fig. 4.

All sources are treated independently. For each, the geocentric ephemerides of the 2000 clone orbits are computed for 30 days, starting at the current epoch with a time step of one day. At each computed epoch, the different orbits result in a cloud of different positions on the sky. The median position with the estimated apparent velocity vector, the convex hull of the cloud, and its angular surface are computed at each time step and stored in a database.

Given the spread in the initial orbital elements, the dispersion of the cloud of predicted positions increases over time. When the search area grows beyond a certain size, a very large field of view or a time-consuming search strategy is required. For this reason, the alerts are considered to be valid only between the epoch of computation and the epoch at which the area on sky becomes larger than five square degrees. If at the first epoch the area is already larger than this threshold, the corresponding alert is skipped and the pipeline processes the following entry on the alert list.

Topocentric ephemerides (for each observatory registered in the system; see below) are then computed. The time step and duration of prediction are adapted to each observatory according to each user's preference (i.e., maximum search area on the sky). Similarly to the geocentric ephemerides, the area, median position, and convex hull of the cloud of predictions are computed for each alert, observatory, and time step, which are stored in a database.

All these predictions are published online through a suite of online portals[5]. A public page lists all the alerts whose area is smaller than one square degree and whose apparent magnitude is brighter than $V = 21$, based on their geocentric ephemerides. For each alert, the dates of release and end of validity are given, together with an identifier[6], the predicted median right ascension (RA) and declination (Dec), the area, and the apparent magnitude. The details of each alert, notably a display of the convex hull of the predictions at each time step with `AladinLite` (Bonnarel et al. 2000), are accessible on specific pages (Fig. 5).

[5] https://gaiafunsso.imcce.fr/

[6] The nomenclature is `gYwNNN`, with `Y` the year of *Gaia* operations, `w` the week of the year, and `NNN` the incremental number of alerts in that week.

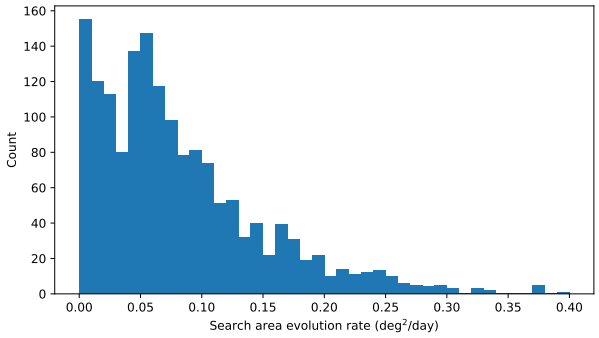


**Fig. 6.** Distribution of the growth rate of the search regions, in $\mathrm{deg}^2\,\mathrm{day}^{-1}$, for all alerts released between November 2016 and July 2020. The median growth rate is $0.06\,\mathrm{deg}^2\,\mathrm{day}^{-1}$, with a standard deviation of $0.08\,\mathrm{deg}^2\,\mathrm{day}^{-1}$.

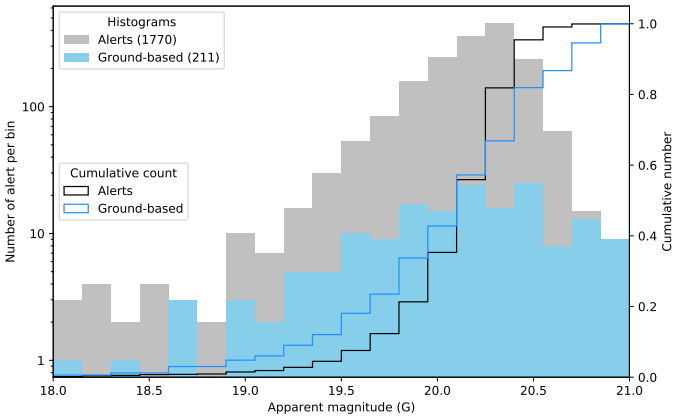


**Fig. 7.** Distribution of the *G* magnitude of all alerts and of ground-based observations.

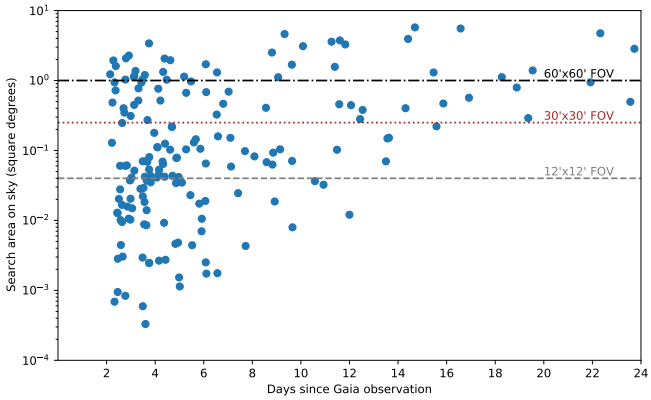


**Fig. 8.** Extent (in square degrees) of the search regions of alerts at the time of their observations by the network, counted in days since *Gaia* observations.

These geocentric predictions are available to everyone. Additional functionalities are provided to registered users. Anyone can register for free in the system by filling out a simple form. Upon registration, users can easily list their observing devices (i.e., observatories). The main characteristics of each device are its location on the Earth – determined by its longitude, latitude, altitude, or International Astronomical Union (IAU) Minor Planet Center (MPC) observing code[7] – its field of view, and the thresholds in apparent magnitude and area on sky to consider for alerts. Hence, for registered users, the list of alerts proposed by the Web pages contains only those fulfilling the user's observability criteria: apparent magnitude brighter than the threshold, area on sky smaller than the threshold, and declination observable from the observatory. Furthermore, the pages presenting the details provide additional features: The `AladinLite` sky view shows the field of view of the device to help prepare the observations (Fig. 5); the convex hull at each time step can be downloaded (to be used in `Aladin` or a user's in-house software); and a simple page is proposed to observers to report on the status of their observation ("success" or "target not found").

## 4. The *Gaia*-FUN-SSO ground-based network

As explained in Sect. 2, the necessity of follow-up observations from ground-based stations was recognized early on. Two aspects, closely related to the specificity of *Gaia*, required multiple stations spread widely over the globe to cover a large range of longitudes and latitudes. First, *Gaia* is an all-sky surveyor, hence requiring follow-up stations in both the northern and southern hemisphere. Second, the strong yet unknown parallax between *Gaia* and the Earth carries a significant uncertainty on the sky coordinates for any new detections (Bancelin et al. 2012), which increases with time (Fig. 6). Observations as early as possible after detection by Gaia are therefore more likely to succeed than delayed ones, necessitating a wide coverage in longitudes.

Before the launch of *Gaia*, efforts were conducted to build this large network. The early assessment of the magnitude range of potential discoveries opened up the possibility of alerts observable with modest apertures (0.5–1 m). Our requests for volunteers were warmly received, and over 150 participants, including amateur astronomers, had registered in the alert release system by the time of *Gaia*'s launch. We consolidated and interacted with the network of volunteers (observations were to be conducted on a best-effort basis) through three workshops, which were held at the Paris Observatory in 2010, 2012, and 2014 (Tanga & Thuillot 2010, 2012, 2014). We also trained the network to react to alerts by releasing calls for observations on NEAs (Thuillot et al. 2015).

However, the contribution of the network has been concentrated in only a few observatories since 2016, with fewer detections per week than foreseen. First, between the early assessment of the *Gaia* capabilities for SSOs in 2007, the start of the *Gaia* operations in 2014, and the effective daily processing of alerts in November 2016 (see below), wide surveys (e.g., Pan-STARRS and WISE) had already discovered most of the SSOs observable by *Gaia* ($V \leq 20.7$). The bulk of alerts hence correspond to objects fainter than $V \approx 20$ (Fig. 7). Telescopes larger than the typical 1 m are therefore required, and cameras with large fields of view are favored, which strongly limits the potential contribution by amateurs. Second, the areas to search increase with time due to the lack of constraints on the short-term orbit (Figs. 6, 8). Owing to delays from multiple sources – the onboard observations, the downlink to Earth, the IDT, and the many steps in the SSO-ST – alerts are released, at the earliest, about 48 h after the observations.

Although this delay may appear long compared to, for example, alerts for gamma ray bursts with the *Swift* telescope (3–8 h; see Barthelmy et al. 2005), the complexity of the prediction for moving objects is much higher: The astrometry measured by *Gaia* cannot be directly used (contrarily to galactic or extragalactic sources), and preliminary orbits must be computed

[7] http://vo.imcce.fr/webservices/data/displayIAUObsCodes.php

**Table 1.** Most actively participating observatories of the network, with their numbers of detections (up to July 2020).

| Observatory | Code | Country | Apert. (m) | Detections |
|---|---|---|---|---|
| Observatoire de Haute Provence (OHP) | 511 | France | 1.2 | 44 |
| C2PU, Observatoire de la Côte d'Azur) | 010 | France | 1.0 | 23 |
| Terskol Observatory | B18 | Ukraine | 0.6 & 2.0 | 27 |
| Kyiv Comet station | 585 | Ukraine | 0.7 | 21 |
| Odessa Mayaki Observatory | 583 | Ukraine | 0.8 | 18 |
| Abastumani Observatory, Tbilisi | 119 | Georgia | 0.7 | |
| Las Cumbres Observatory Global Telescope Network | V37 | USA | 1.0 | 113 |
| | V39 | USA | 1.0 | |
| | W85 | Chile | 1.0 | |
| | W86 | Chile | 1.0 | |
| | W87 | Chile | 1.0 | |
| | Q63 | Australia | 1.0 | |
| | Q64 | Australia | 1.0 | |
| | K91 | South Africa | 1.0 | |
| | K92 | South Africa | 1.0 | |
| | K93 | South Africa | 1.0 | |

(Sect. 2). However, considering that *Gaia* was designed as a long-term stellar mapper, the availability of alerts 48 h after the observations can be considered as an achievement. Nevertheless, the area and its evolution with time are strongly tied to the number of transits observed by *Gaia*. With increasing delays, it is often required that observers scan the area to search with multiple exposures as the area becomes larger than their instrument field of view.

Although that fact limited the kind of facilities participating in the network, the numerous discoveries by other surveys did not reduce interest in the SSO-ST. First, *Gaia*, being an all-sky survey observing at solar elongation between 45° and 135°, provides the opportunity to discover SSOs in the region of the sky poorly covered by ground-based telescopes. Second, SSOs with poorly characterized orbits are likely not recognized and hence are processed by the SSO-ST as new sources. Observations by the network provide new constraints that improve their orbit, allowing the Minor Planet Center (MPC) to link them with known SSOs and hence a subsequent identification by *Gaia* or by ground-based observatories.

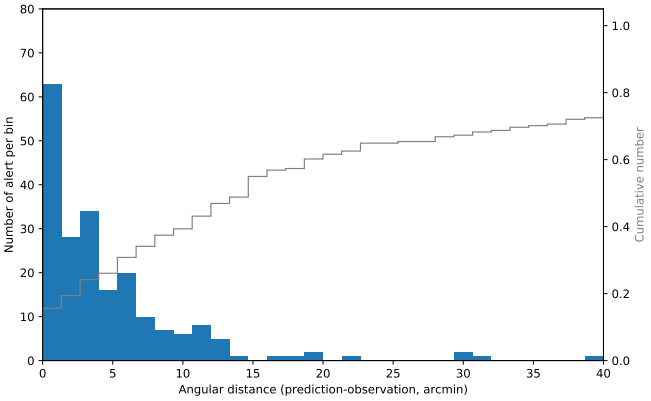


**Fig. 9.** Distribution of the angular distance between the predicted median (RA, Dec) coordinates and the observed position measured from the ground (solid bar). The cumulative distribution of the ephemeris uncertainty (reported as the square root of the sky area) is also reported (gray line). Objects are typically found well within the uncertainty.

## 5. Results

Soon after the start of *Gaia*'s regular operations in September 2014[8], the SSO-ST faced several issues that did not materialize in the pre-launch simulations. The issue that most delayed the release of alerts was the number of contaminants, several orders of magnitude above expectations. Filtering these contaminants required several cycles of tests and adaptations of the SSO-ST pipeline such that the pipeline did not become fully functional until November 2016, which was a delay of 24 months with respect to expectations. Since then, the pipeline has been very robust, running continuously on the computation facilities of the Centre National d'Etudes Spatiales (CNES), in Toulouse, France, with the exception of a few technical interruptions. It has also proved to produce a clean set of alerts in the output, effectively rejecting the contaminants.

Since the start of the automated operations, more than 1700 alerts have been released. Observations from the ground have been performed for almost 250 of them, leading to the successful observation of 227 *Gaia* discovery candidates. Most of these observations were performed by a small number of observatories (Table 1) and an even smaller number of astronomers; the observations at C2PU (Centre Pédagogique Planète Univers), OHP (Observatoire de Haute Provence), and the Las Cumbres Observatory Global Telescope (LCOGT) were carried out by the same observers as part of a concerted effort to follow up on alerts from *Gaia* – for SSOs, as described here, but also for photometric alerts (e.g., Simon et al. 2019).

This limited number of participants with respect to the large network built before the launch is the result of two effects. First, the delay between the launch of *Gaia* and the starting date of alert releases lowered the interest of observers in the alerts. Second, the distribution of apparent magnitude and area of sky (Figs. 7 and 8) limited the participants to those using large aperture telescopes with optical configurations that provide large fields of view.

As such, most of the ground-based follow-up has been performed by the co-authors of the present article. Early observations were mainly performed at the OHP 1.2-m telescope,

[8] The scanning law during the first three months, called the ecliptic pole scanning law (EPSL), was different (Clementini et al. 2016).

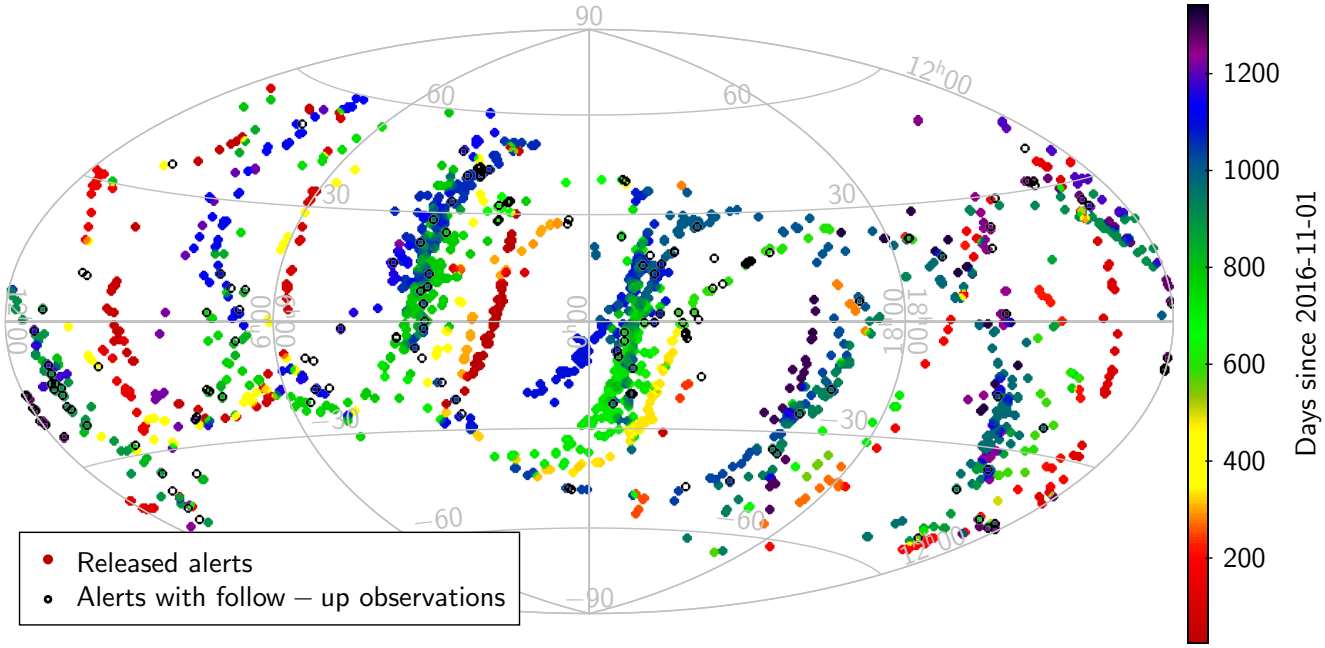


**Fig. 10.** Distribution of the alerts in equatorial coordinates (dots, color coded by epoch), together with the ground-based observations (open circles). The black line represents the ecliptic plane. The pattern is a combination of the distribution of asteroids (with almost no objects close to ecliptic poles) and *Gaia*'s scanning law (following great circles). The gaps correspond to epochs when the SSO-ST was not yet in operation.

the field of view ($12' \times 12'$) of which seldom covered the entire search region. Hence, we had to scan the search area with multiple exposures, slowing the process. We soon started to use the C2PU 1-m telescope, whose field of view ($38' \times 38'$) was more adapted to our needs. The successful recovery of the alerts g1P024 and g1j03C (2012 $VR_{82}$) at these telescopes in 2017 showed that the pipeline was delivering real SSO alerts that could be confirmed from the ground, starting from the receipt of the alert up to almost ten days after (Carry et al. 2019).

While the number of recoveries increased, we noted that most objects were found well within the search area, on average at only $3'$ from the median of the predicted coordinates (Fig. 9). In other words, the area in the sky of the alerts can be large, but the reported medians (RA, Dec) are good estimators of the positions. This results from the orbital distribution of alerts (see Carry 2014, and Sect. 6). The majority of SSOs to be discovered orbit in the main asteroid belt. However, because the distance of the SSO is not known at the time of detection, the orbital elements may cover a wide range of semimajor axes, resulting in highly different apparent motions that cause the sky area to increase. However, the bulk of detections consist of main-belt asteroids, to which the median coordinates correspond. This explains the apparent contradiction between the large sky area (uncertainty) and the well-approximated coordinates.

Therefore, we continued to observe with the 1.2-m telescope at the OHP. Following these first recoveries, the number of successfully observed alerts dramatically increased with the use of the LCOGT network, which offers 1-m telescopes with large fields of view ($27' \times 27'$) located all over the Earth, hence perfectly adapted to the distribution of alerts on the celestial sphere (Fig. 10) and to the large search area.

For each alert, we always test whether the ground-based observation corresponds to the object detected by *Gaia*. To this end, we compute an orbit based on both the *Gaia* transits and the ground-based astrometry (the latter measured with the *Gaia* Ground Based Optical Tracking software; Bouquillon et al. 2014). We use a modified version of `OrbFit` (Orbfit Consortium 2011), which was used to validate the astrometry of SSOs in *Gaia* DR2 (Spoto et al. 2018). For each successful recovery, we send both the ground-based and *Gaia* astrometry to the MPC. The astrometry of unconfirmed alerts has been not been automatically sent to MPC (up to the time of writing). Finally, the astrometry of known objects is not sent daily to the MPC, but is released in batches at the time of *Gaia* DRs (e.g., DR2, Spoto et al. 2018) to benefit from the high-precision attitude of the satellite.

The MPC has been collecting the minor planet astrometry acquired worldwide for decades. Upon reception of the astrometry of an unidentified object, such as a *Gaia* alert, the MPC tries to link it with known objects based on its observation database, including the unpublished portion. Several cases are possible: The alert can correspond to a new, never before observed object, an object recently detected by another observatory and not yet ingested by the `astorb` database, or a known object with a poorly determined orbit (which precluded its identification within the SSO-ST and from the ground).

The MPC is the sole international organization collecting astrometry, and we rely on it entirely to determine if the *Gaia* alerts were hitherto unknown objects or recoveries of newly or poorly characterized SSOs. The "results"[9] page of the *Gaia*-FUN SSO Web interface lists the designations of all recovered alerts. Of the 250 follow-up observations, 139 have received a designation, but only six are attributed to *Gaia* (2018 $XL_{20}$, 2018 $XL_4$, 2018 $YK_4$, 2018 $YM_4$, 2019 $CZ_{10}$, and 2019 $HO_4$). However, the others were poorly characterized SSOs, and their observation in the context of the *Gaia*-FUN-SSO drastically improved their orbital elements.

## 6. Orbital distribution

We use the designations assigned by the MPC to retrieve the orbital elements of the SSOs that led to alerts. We compare their

[9] https://gaiafunsso.imcce.fr/stats/network.php

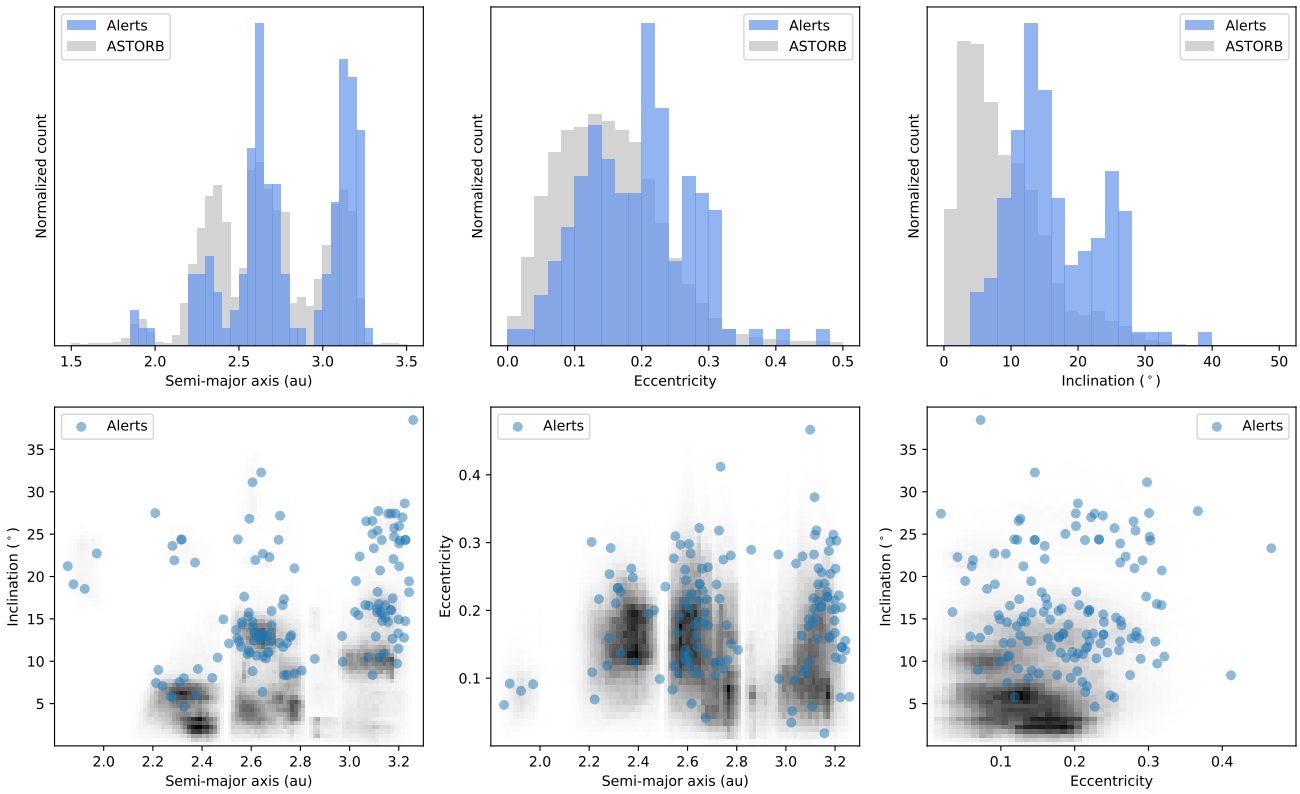


**Fig. 11.** Comparison of the distribution of the detected asteroids with the current census of SSOs as represented by the `astorb` database.

distribution in semimajor axis, eccentricity, and inclination in Fig. 11.

As of July 2020, all the recovered *Gaia* alerts concerned main-belt asteroids. Considering that 139 alerts were assigned a designation and that the incidence of NEAs was expected to be 1–2%, this is not surprising. Moreover, the SSO-ST may be biased against NEAs for several reasons. First, as NEAs present a higher apparent motion than main-belt asteroids, they will smear and move faster outside the transmitted windows. Their transits will hence contain fewer observations, which may lead to the rejection of the transit at the DU454 level. Second, their motion combined with the *Gaia* scanning law may result in fewer overall transits, leading to more rejections of NEAs at the DU459 level. We can, however, attest to the SSO-ST capability of processing NEAs: we injected real *Gaia* observations of known NEAs into the SSO-ST, and the pipeline produced alerts (that we did not release) centered on the real location of the targets, with sky areas typical of the SSO-ST.

Regarding the distribution of orbital elements, the sample of alerts is different from the current census of asteroids taken from `astorb`. We applied a 1D Kolmogorov-Smirnov (K-S) test to the semimajor axis, eccentricity, and inclination in turn (Fig. 11, top line) to test whether the distributions from the alerts and from `astorb` are similar; this resulted in K-S p-values of $10^{-4}$, $10^{-9}$, and $10^{-33}$, respectively. These values are well below the typical threshold of 0.2 for similar distributions, and therefore we find it highly unlikely that the distributions are similar.

The alerts are typically located in the outer main belt and have more inclined and more eccentric orbits than the known population (Fig. 11, bottom line). There is a weak correlation between the semimajor axis and inclination (hence alerts are preferentially for high-inclination outer main-belt asteroids). We explored the potential correlations between the apparent characteristics of the alerts (e.g., equatorial coordinates, apparent $G$ magnitude, and apparent rate) and the orbital elements and found none. We did not uncover any clear detection bias due to *Gaia*. This is not unexpected as half of the alerts are brighter than $G = 20.1$ mag (Fig. 7), well within the limiting magnitude of *Gaia*.

The outer main belt being farther, and populated by darker asteroids, than the inner parts of the belt, its completeness at a given size is lower (DeMeo & Carry 2013). The bias in the current census against high-inclination orbits has already been reported by Mahlke et al. (2018) based on deep images obtained by the Kilo-Degree Survey (KiDS). In the present article, the distribution of alerts clearly skewed toward high inclinations highlights the strength of *Gaia*'s all-sky survey. With the final release of the SSO catalog by *Gaia*, efforts to debias the current census of SSOs will be possible.

## 7. Conclusion

Since the beginning of *Gaia*'s operations in 2014, a specific pipeline has been running daily to process the unidentified SSOs observed by *Gaia*. Since 2016, about 1700 calls for observations, called alerts, have been released to trigger ground-based follow-up observations of these unidentified objects. Among these, 250 recovery observations have been attempted, resulting in the detection of 227 of them. Their astrometry has been sent to the MPC, which assigned a preliminary designation to 139 of these objects, including six attributed to *Gaia*. The orbital distribution of these alerts confirms the bias in the current census of the asteroid population against highly inclined objects. This bias is even more pronounced in the outer asteroid belt.

The daily processing pipeline is still running and will continue until the end of *Gaia*'s operations, which have been

extended to the end of 2022 by ESA, and possibly until the end of 2024 (approval pending).

*Acknowledgements.* We are indebted to the engineers of the European Space Agency and of the Data Processing Center CNES in Toulouse, France, who made possible this mission and these observations. We thank CNRS-INSU (France) and the scientific council of the *Gaia* observing service ANO1 for the yearly funding allowing us to observe periodically at Haute-Provence Observatory (OHP). We thank the referee J.J. Kavelaars for his comments. This work presents results from the European Space Agency (ESA) space mission *Gaia*. *Gaia* data are being processed by the *Gaia* Data Processing and Analysis Consortium (DPAC). Funding for the DPAC is provided by national institutions, in particular the institutions participating in the *Gaia* MultiLateral Agreement (MLA). The *Gaia* mission website is https://www.cosmos.esa.int/gaia. The *Gaia* archive website is https://archives.esac.esa.int/gaia. RAM acknowledges support from CONICYT/FONDECYT Grant No. 1190038 and from the Chilean Centro de Excelencia en Astrofisica y Tecnologia as Afines (CATA) BASAL PFB/06. We are grateful for the continuous support of the Chilean National Time Allocation Committee under programs CN2019A-3, CN2019B-16, and CN2020A-20. We thank all the observers participating in this program. This work has financially been supported by Agenzia Spaziale Italiana (ASI) through contracts I/037/08/0, I/058/10/0, 2014-025-R.0. The observations at Abastumani were supported by the Shota Rustaveli National Science Foundation, Grant RF-18-1193.

## References

Bailen, M., Moskovitz, N., Burt, B., Wasserman, L., & Schottland, R. 2020, in 51st Lunar and Planetary Science Conference, 51, 2078
Bancelin, D., Hestroffer, D., & Thuillot, W. 2012, Planet. Space Sci., 73, 21
Barthelmy, S. D., Barbier, L. M., Cummings, J. R., et al. 2005, Space Sci. Rev., 120, 143
Berthier, J., Vachier, F., Thuillot, W., et al. 2006, in Astronomical Society of the Pacific Conference Series, 351, Astronomical Data Analysis Software and Systems XV, eds. C. Gabriel, C. Arviset, D. Ponz, & S. Enrique, 367
Berthier, J., Carry, B., Vachier, F., Eggl, S., & Santerne, A. 2016, MNRAS, 458, 3394
Bonnarel, F., Fernique, P., Bienaymé, O., et al. 2000, A&AS, 143, 33
Bouquillon, S., Barache, C., Carlucci, T., et al. 2014, Proc. SPIE, 9152, 915203
Bowell, E. 2014, vizier.u-strasbg.fr/viz-bin/VizieR-2
Carry, B. 2014, in Gaia-FUN-SSO Workshop 2014
Carry, B., Spoto, F., Thuillot, W., et al. 2019, in EPSC-DPS Joint Meeting 2019, 13, 1409-1, 2019
Clementini, G., Ripepi, V., Leccia, S., et al. 2016, A&A, 595, A133
Cropper, M., Katz, D., Sartoretti, P., et al. 2018, A&A, 616, A5
DeMeo, F. E., & Carry, B. 2013, Icarus, 226, 723
Fabricius, C., Bastian, U., Portell, J., et al. 2016, A&A, 595, A3
Fedorets, G., Muinonen, K., Pauwels, T., et al. 2018, A&A, 620, A101
Gaia Collaboration (Brown, A. G. A., et al.) 2016a, A&A, 595, A2
Gaia Collaboration (Prusti, T., et al.) 2016b, A&A, 595, A1
Ivezić, Ž., Tabachnik, S., Rafikov, R., et al. 2001, AJ, 122, 2749
Jordi, C., Gebran, M., Carrasco, J. M., et al. 2010, A&A, 523, A48
Mahlke, M., Bouy, H., Altieri, B., et al. 2018, A&A, 610, A21
Mignard, F., Cellino, A., Muinonen, K., et al. 2007, Earth Moon Planets, 101, 97
Muinonen, K., Fedorets, G., Pentikäinen, H., et al. 2016, Planet. Space Sci., 123, 95
Orbfit Consortium 2011, OrbFit: Software to Determine Orbits of Asteroids
Perryman, M. A. C., de Boer, K. S., Gilmore, G., et al. 2001, A&A, 369, 339
Riello, M., De Angeli, F., Evans, D. W., et al. 2018, A&A, 616, A3
Rudenko, M. 2016, in Asteroids: New Observations, New Models, Proc. IAU Symp., 318, 265
Simon, A., Pavlenko, E., Shugarov, S., et al. 2019, Contrib. Astron. Observ. Skalnate Pleso, 49, 420
Spoto, F., Del Vigna, A., Milani, A., et al. 2018, A&A, 614, A27
Tanga, P. 2011, in Solar System Science Before and After Gaia, 2
Tanga, P., & Thuillot, W., 2010, Proceedings of the Gaia-FUN SSO workshops, IMCCE, Paris Observatory
Tanga, P., & Thuillot, W., 2012, Proceedings of the Gaia-FUN SSO Workshops, IMCCE, Paris Observatory
Tanga, P., & Thuillot, W., 2014, Proceedings of the Gaia-FUN SSO Workshops, IMCCE, Paris Observatory
Tanga, P., Mignard, F., Dell'Oro, A., et al. 2016, Planet. Space Sci., 123, 87
Thuillot, W., & Dennefeld, M. 2018, in SF2A-2018: Proceedings of the Annual meeting of the SF2A, eds. P. Di Matteo, F. Billebaud, F. Herpin, N. Lagarde, J. Marquette, A. Robin, & O. Venot, 463–465
Thuillot, W., Bancelin, D., Ivantsov, A., et al. 2015, A&A, 583, A59

[1] Institut de Mécanique Céleste et de Calcul des Éphémérides IMCCE, Observatoire de Paris, Université PSL, CNRS, Sorbonne Université, Université de Lille, 77 av. Denfert Rochereau, 75014 Paris, France
[2] Université Côte d'Azur, Observatoire de la Côte d'Azur, CNRS, Laboratoire Lagrange, Boulevard de l'Observatoire, CS34229, 06304, Nice Cedex 4, France
e-mail: benoit.carry@oca.eu
[3] Harvard-Smithsonian Center for Astrophysics, 60 Garden St., MS 15, Cambridge, MA 02138, USA
[4] SYRTE, Observatoire de Paris, PSL Research University, CNRS, Sorbonne Université, UPMC Univ. Paris 06, LNE, 61 avenue de l'Observatoire, 75014 Paris, France
[5] Departamento de Astronomía, Facultad de Ciencias Físicas y Matemáticas, Universidad de Chile, Casilla 36-D, Santiago, Chile
[6] Aix Marseille University, CNRS, Institut Pytheas-Observatoire Haute Provence, 04870 St-Michel-l'Observatoire, France
[7] INAF – Osservatorio Astrofisico di Arcetri, Largo Enrico Fermi 5, 50125 Firenze, Italy
[8] Department of Physics, Gustaf Hällströmin katu 2, University of Helsinki, PO Box 64, 00014, Finland
[9] Astrophysics Research Centre, School of Mathematics and Physics, Queen's University Belfast, Belfast BT7 1NN, UK
[10] CNES Centre Spatial de Toulouse, 18 avenue Edouard Belin, 31401 Toulouse Cedex 9, France
[11] Asteroid Engineering Lab, Onboard Space Systems, Luleå University of Technology, Box 848, 981 28 Kiruna, Sweden
[12] Finnish Geospatial Research Institute, Geodeetinrinne 2, 02340, Masala, Finland
[13] Royal Observatory of Belgium, Avenue Circulaire 3, 1180 Bruxelles, Belgique
[14] Observatoire de Besançon, UMR CNRS 6213, 41 bis avenue de l'Observatoire, 25000, Besançon, France
[15] Kharadze Abastumani Astrophysical Observatory, Ilya State University, K. Cholokashvili Avenue 3/5, Tbilisi 0162, Georgia
[16] Samtskhe-Javakheti State University, Rustaveli Street 113, Akhaltsikhe 0080, Georgia
[17] Astronomical Observatory, Taras ShevChenko National University of Kyiv, 3 Observatorna str., Kyiv, 04053, Ukraine
[18] Institut d'Astrophysique de Paris, Sorbonne Université, CNRS, UMR 7095, 98 bis bd Arago, 75014, Paris, France
[19] Institut Polytechnique des Sciences Avancées IPSA, 63 bis Boulevard de Brandebourg, 94200 Ivry-sur-Seine, France
[20] Vera C. Rubin Observatory/DIRAC Institute, Department of Astronomy, University of Washington, 15th Ave. NE, Seattle, WA 98195, USA
[21] ICAMER Observatory of NASU, 27 Acad. Zabolotnogo str., Kyiv, 03143, Ukraine
[22] Astronomical Observatory of Odessa I.I. Mechnikov National University, 1v Marazlievska str., Odessa, 65014, Ukraine
[23] Institute of Astronomy, V.N. Karazin Kharkiv National University, Sumska Str. 35, Kharkiv, 61022, Ukraine
[24] Keldysh Institute of Applied Mathematics, RAS, Miusskaya sq. 4, Moscow, 125047, Russia
[25] Astronomy and Space Physics Department, Taras Shevchenko National University of Kyiv, 60 Volodymyrska str., Kyiv, 01601, Ukraine
[26] National Center "Junior Academy of Sciences of Ukraine", 38-44, Degtyarivska St., Kyiv, 04119 , Ukraine
[27] Terskol Branch of INASAN RAN, 48 Pyatnitskaya str., Moscow, 119017, Russia
[28] LESIA, Observatoire de Paris, Sorbonne Université, Université PSL, CNRS, Univ. Paris Diderot, Sorbonne Paris Cité, 5 place Jules Janssen, 92195 Meudon, France
[29] naXys, University of Namur, Rempart de la Vierge, Namur 5000, Belgium
[30] Astronomical Observatory Institute, Faculty of Physics, A. Mickiewicz University, Słoneczna 36, 60-286 Poznań, Poland